Design of Potent, Selective, and Orally Bioavailable Inhibitors of Cysteine Protease Cathepsin K

Francis X. Tavares,*,† Virginia Boncek,‡,§ David N. Deaton,† Anne M. Hassell,∥ Stacey T. Long,⊥ Aaron B. Miller,∥ Alan A. Payne,‡ Larry R. Miller,‡ Lisa M. Shewchuk,∥ Kevin Wells-Knecht,△ Derril H. Willard Jr.,⊗,○ Lois L. Wright,▽ and Hui-Qiang Zhou†

Department of Medicinal Chemistry, Discovery Research Biology, Department of Research Bioanalysis and Drug Metabolism, Discovery Research CASS, Department of Molecular Pharmacology, Preclinical Development, and Department of Gene Expression and Protein Biochemistry, GlaxoSmithKline, Research Triangle Park, North Carolina, 27709

Received August 5, 2003

Osteoclast-mediated bone matrix resorption has been attributed to cathepsin K, a cysteine protease of the papain family that is abundantly and selectively expressed in osteoclast. Inhibition of cathepsin K could potentially be an effective method to prevent osteoporosis. Structure−activity studies on a series of reversible ketoamides based inhibitors of cathepsin K have led to identification of potent and selective compounds. Crystallographic studies have given insights into the mode of binding of these inhibitors. A series of ketoamides with varying P1 moieties were first synthesized to find an optimum group that would fit into the S1 subsite of the cysteine protease, cathepsin K. With a desired P1 group in place a variety of heterocyclic analogues in the P′ region were synthesized to study their steric and electronic effects. In the process of exploring these P′ heterocyclic variations, excellent selectivity was gained over other highly homologous cysteine proteases, including cathepsins L, S, and V. The favorable pharmacokinetic properties of some of these cathepsin K inhibitors in rats make them suitable for evaluation in rodent osteoporosis models. A representative cathepsin K inhibitor was shown to attenuate PTH-stimulated hypercalcemia in the TPTX rat model. These inhibitors provide a viable lead series in the discovery of new therapies for the prevention and treatment of osteoporosis

Introduction

Bone metabolism, consisting of bone formation and resorption is a dynamic process in life, and balance of these opposing processes is necessary for the preservation of skeletal mass and architecture. A shift in the balance of this dynamic process can lead to abnormalities in bone mass. Osteoporosis is a disease characterized by generalized skeletal fragility resulting in fractures occurring with minimal trauma. Bone remodeling involves osteoclast-mediated dissolution of bone mineral as well as degradation of its protein matrix. Osteoclasts form an extracellular compartment by firmly attaching to the bone surface. This attachment allows the establishment of an acidic environment that facilitates demineralization of the bone.[1] Osteoclasts then secrete proteolytic enzymes into this compartment to degrade the organic matrix. Cysteine proteases have been implicated in this osteoclast-mediated resorption on the bone matrix. The expression of cathepsin K, a cysteine protease of the papain superfamily, is abundant and selective in osteoclasts, suggesting that this enzyme is crucial for bone resorption.[2a,b] Cathepsin K antisense nucleotide studies have implicated this enzyme in osteoclast-mediated bone resorption.[3] In addition, a link between mutations in human cathepsin K and pycnodysostosis, a rare osteopetrotic disease characterized by abnormal bone resorption, has been demonstrated.[4] Recently, it has also been shown that cathepsin K-deficient mice exhibit a distinct osteopetrotic phenotype.[5] Recent work has shown that cathepsin K, and not cathepsin L, is the major protease responsible for human osteoclastic bone resorption.[6] The effects of a small molecule inhibitor of cathepsin K has also been evaluated on bone resorption in vivo using a nonhuman primate model of postmenopausal bone loss in which the active form of cathepsin K is identical to the human ortholog. These studies suggest that selective inhibition of cathepsin K could provide an effective therapy for the treatment of osteoporosis.

Cysteine proteases make up the vast majority of lysosomal proteases. There are currently 11 members of the human cathepsin cysteine protease family. With the exception of cathepsin K, the physiological role and pathological implications of many cathepsins are not well understood. Cysteine proteases such as Cathepsins B, S, and L have been implicated in im-

* To whom correspondence should be addressed. Phone: (919) 483-7456; Fax: (919)-483-6053; e-mail: fxt66911@gsk.com.
† Department of Medicinal Chemistry.
‡ Department of Molecular Pharmacology.
§ Present address: 3040 Cornwallis Rd., 111 Hermann Building, Research Triangle Park, NC 27709.
∥ Discovery Research CASS.
⊥ Preclinical Development.
△ Department of Research Bioanalysis and Drug Metabolism.
⊗ Department of Gene Expression and Protein Biochemistry.
○ Deceased.
▽ Discovery Research Biology.

10.1021/jm030373l CCC: $27.50
Published on Web 12/24/2003

Scheme 1

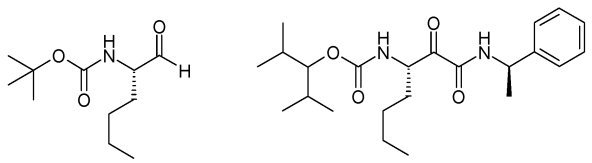

1 2

munological responses.[8,9] Cathepsin B, for example, is the most abundant lysosomal cysteine protease implicated in the pathogenesis of rheumatoid arthritis, muscular dystrophy, and tumor metastasis.[7] Cathepsins V and S are more tissue specific with cathepsin V expressed in thymus, and cathepsin S in spleen and lung.[8−10] Cathepsins S and L have been implicated in major histocompatibility complex (MHC) class II invariant chain processing.[8,9] In lieu of the fact that cathepsins L, S, V, and K have a high degree of homology, design of inhibitors that are selective for the inhibition of cathepsin K is challenging. The difficulty in designing selective cathepsin inhibitors results from the similarity in their substrate recognition as well as their common proteolytic mechanism.[10b] Since the treatment of osteoporosis would require chronic administration of a drug, the development of a selective reversible inhibitor was desired. This could potentially avoid antigenicity due to covalent modification of proteins via irreversible inhibition. Numerous warheads have been utilized in reversible inhibitors of cysteine proteases including peptidic aldehydes,[11] nitriles,[12] cyclopropenones,[13] diamino ketones,[14] and α-ketoamides.[15] There has also been a recent report on the use of noncovalent amides as cathepsin K inhibitors.[16] This group was particularly interested in exploring α-ketoamides as reversible inhibitors of cathepsin K. The ketoamide class of inhibitors has been widely employed in inhibiting serine proteases.[15,17] Herein is described its use in the inhibition of the cysteine protease, cathepsin K. Synthetic efforts in these laboratories focused around the ketoamide inhibitor **2** (cathepsin K IC_{50} = 2.54 nM) which was derived from the peptide aldehyde lead **1** (cathepsin K IC_{50} = 51 nM). The aim was to optimize on the structural and physiochemical features of **2** by examining changes in the P_1 amino acid of the ketoamide as well as studying the role of P′ electron deficient heterocycles in modulating the electrophilicity of the warhead. In the process of these P′ heterocyclic replacements, the achievement of selectivity over other cysteine proteases was obtained and will be discussed. In addition to in vitro SAR studies, the evaluation of certain compounds in pharmacokinetic and pharmacodynamic studies in the rat will be described.

Chemistry. The general syntheses of ketoamide inhibitors are shown in Scheme 2. The alcohol **3** was treated with phosgene to afford a chloroformate, and subsequent addition of an amino ester provided carbamates **4**.[18] Hydrolysis of esters **4** to acids followed by coupling with the phosphorane afforded cyanoylides **5**. Oxidation of the ylide **5** following the Wassermann procedure[19] and trapping the acyl nitrile with amines afforded the ketoamides **6**−**43**. The 1-alkyl-1*H*-pyrazole-5-ylamines (**26a**−**32a**) and the amines **34a**, **35a**, and **36a** were synthesized following literature procedures.[20−22]

Results and Discussion

Previous efforts in these laboratories had identified the P1 *n*-butyl substituent, derived from commercially available norleucine, as a potency enhancing group for aldehyde-based inhibitors. Since changing the thiol reactive group might modify the P1 SAR, P1 analogues in the ketoamide series were synthesized. The IC_{50} values are the mean of two or three inhibition assays, individual data points in each experiment were within 3-fold range of each other. Cathepsin K inhibition data for the P_1 modification are shown in Table 1. The glycine-derived analogue **6**, lacking a chiral center (R = H), was found to be a weak inhibitor (IC_{50} > 12 μM). Introduction of a substituent on the carbon adjacent to the ketone can bias the preferred rotational conformer of the inhibitor as well as providing opportunities for additional binding interactions. The methyl analogue **7** exhibits enhanced potency (IC_{50} = 360 nM). Some of this increase may arise from a lower entropic cost of binding due to stabilization of the active rotamer. Increasing the size of the substituent at P1 with amino acids valine, leucine, isoleucine, phenylalanine, and norleucine gave analogues **8**−**10** and **12** and **13**, respectively. These modifications gave a boost in potency, with compound **13** being the most potent (IC_{50} = 9.2 nM) in this series of ketoamides. The cyclohexylmethyl analogue **11**, the saturated version of the phenylalanine derivative, was also a potent inhibitor of cathepsin K (IC_{50} = 14 nM). On the basis of these results and desiring to control cost of goods of any potential drug candidate by limiting synthetic complexity, the norleucine-derived *n*-butyl group was selected as an appropriate P1 moiety.

Scheme 2[a]

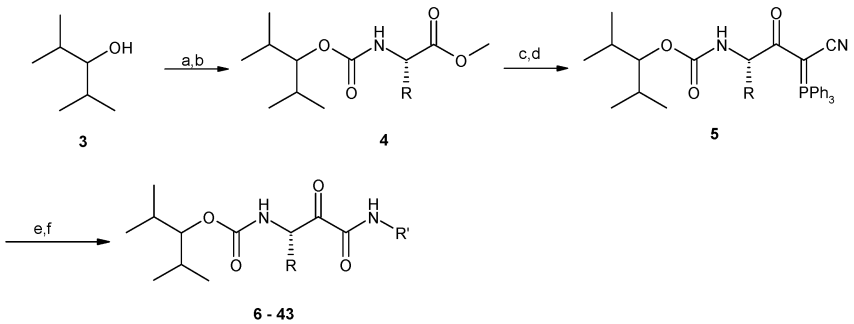

3 4 5 6 - 43

[a] (a) 20% $COCl_2$ in toluene, THF, rt; (b) L-norleucine methyl ester hydrochloride, Hunig's base, THF, rt; (c) 1 M LiOH/THF (1:1), rt; (d) (triphenylphosphoranylidene)acetonitrile, EDCI, DMAP, DCM, rt; (e) ozone, DCM, −78 °C, 15 min.; (f) amine, 1 M $AgNO_3$/THF (1:5), rt.

Table 1. Inhibitory Potencies vs Human Cathepsin K

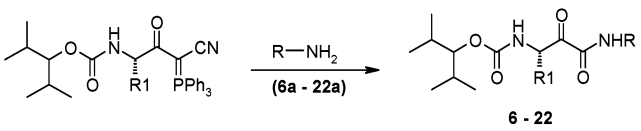

Cmpd	R	R1	IC50 (nM)
6	 **6a**	H	12,000
7	 **7a**	CH_3	360
8	 **8a**	^{i}Pr	47
9	 **9a**	^{i}Bu	24
10	 **10a**	Sec-Bu	87
11	 **11a**	$CH_2C_6H_{11}$	14
12	 **12a**	CH_2Ph	27
13	 **13a**	n-Bu	9.2
14	 **14a**	n-Bu	32
15	 **15a**	n-Bu	95
16	 **16a**	n-Bu	52
17	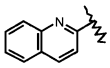 **17a**	n-Bu	250
18	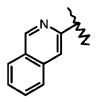 **18a**	n-Bu	4.8
19	 **19a**	n-Bu	40
20	 **20a**	n-Bu	83
21	 **21a**	n-Bu	5.1
22	 **22a**	n-Bu	0.77

The cysteine cathepsins contain a highly conserved tryptophan in the S′ pocket of the active site. Designing ketoamide inhibitors that would take advantage of the interactions with ^{184}Trp in the cathepsin K substrate binding groove would be highly desirable to enhance potency. To this end, various five- and six-membered heterocyclic P′ groups were incorporated into the ketoamide inhibitors with the hope that they might $\pi-\pi$ stack with the indole side chain of ^{184}Trp or form hydrogen bonds with its indole NH.

The six-membered P′ heterocycles, compounds **14**−**16** exhibited less inhibitory activity than the lead compound **2**, with the pyridine analogue **14** (IC_{50} = 32 nM) being the most potent. Incorporation of another nitrogen as in the pyrazine analogue **16** did not boost activity. Fusion of another aryl ring as in the isoquinoline **18** provided a 4-fold enhancement in potency. The site of ring attachment proved crucial with the quinoline **17** being 30-fold less active. This increase in inhibitory activity with the bicyclic system **18** could result from interactions with the tryptophan moiety.

The five-membered P′ heterocycles **19**−**22** proved to be more promising than their corresponding six-membered congeners **14**−**16**. In the five-membered heterocyclic series it was found that heterocycles having a potential hydrogen bond acceptor, as in compounds **19**−**22**, were very potent reversible inhibitors of cathepsin K. The isoxazole **21** was as potent as the lead **2** and the pyrazole **22** was an even better inhibitor. The thiazole **19** and the thiadiazole **20** were significantly less potent. It is difficult rationalizing this potency on the steric or electronic properties of these heterocycles. Insights into the binding of these heterocycles was obtained from an X-ray cocrystal structure of compound **22** bound to cathepsin K at 2.2 Å resolution (Figure 1). The pyrazole has two interactions with the protein: one through a two water interaction to ^{18}Gln and another with ^{184}Trp. The S1 pocket forms a "face" using backbone atoms as well as ^{64}Gly and ^{65}Gly. The norleucine is in the S1 groove with one face and the end exposed to solvent. One of the isopropyl groups is bound in the S2 pocket formed by residues ^{67}Tyr, ^{68}Met, ^{134}Ala, ^{163}Ala, and ^{209}Leu of cathepsin K. From the residues that make up this pocket, it is clear why hydrophobic groups are well tolerated. The other isopropyl group projects in the direction of S3 pocket but does not occupy it. A covalent interaction is made between pyrazole **22** and the protein. The formation of a hemithioketal between ^{25}Cys and the carbonyl of the ketoamide is observed. This is consistent with a reversible transition state inhibitor. However, what is interesting is that the resulting OH of the hemithioketal is not directed into the anionic hole of the protein. The OH interacts with ^{162}His that is part of the catalylic triad, as well as the backbone carbonyl of ^{161}Asn. This represents attack of the thiol in the opposite stereochemistry from previously reported cathepsin K cocrystal structures.[14b,d] The oxyanionic hole is filled by the amide carbonyl of the ketoamide and interacts with the backbone NH of ^{25}Cys and the side chain of ^{19}Gln. Peptidic recognition site interactions are formed between the NH and carbonyl of the inhibitor carbamate group to the backbone carbonyl of ^{161}Asn and the backbone HN of ^{66}Gly, respectively.

Extrapolating the X-ray data from pyrazole **22**, the enhanced potency of analogues **14** and **16** compared to pyridine **15** may be explained by the possible hydrogen bond formation with ^{184}Trp.

From X-ray information of **22**, one could also speculate that in compounds **19**−**21** the lone pair on the nitrogen forms a hydrogen bond with ^{184}Trp. The fact that isoxazole **21** is over 8-fold more active than thiazole

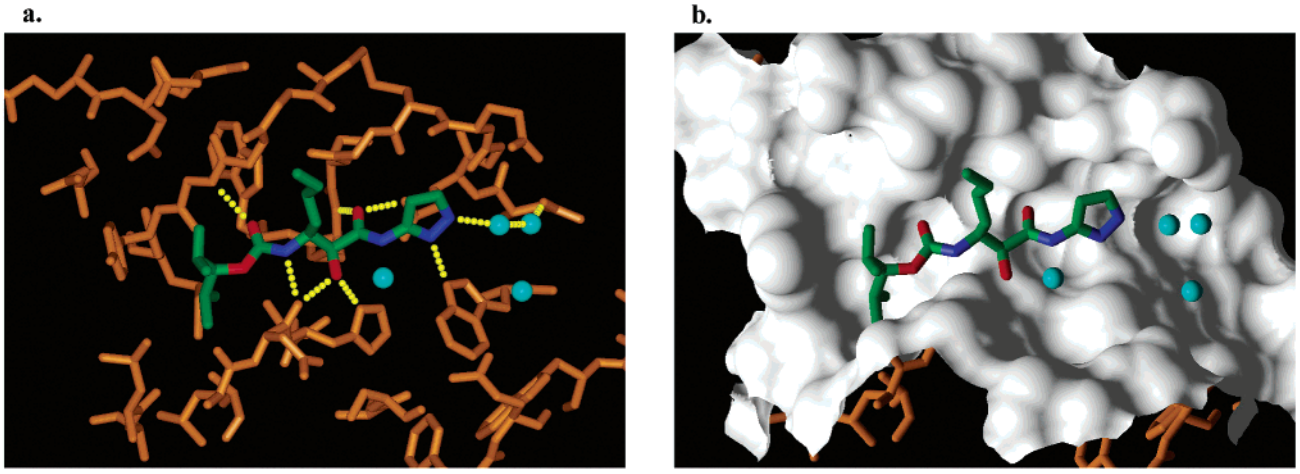

Figure 1. X-ray cocrystal structure of compound **22** bound to cathepsin K at 2.2 Å. Cathepsin K is colored orange, compound **22** by atom type, and critical waters are cyan colored spheres. (a) Active site with hydrogen bonds of the complex highlighted in yellow bonds and (b) surface of active site of cathepsin K. Figure made with the PYMOL program (Delano Scientific, www.pymol.org).

19 and thiadiazole **20** may reflect its ability to form multiple or stronger hydrogen bonds than its congeners, but their drop in potency could also arise from detrimental lone pair interactions of their differentially substituted rings.

Prior to the solution of the X-ray cocrystal structure of pyrazole **22**, the *N*-methylpyrazole analogues **23** and **24** were synthesized to explore the importance of the pyrazole NH in its enhanced inhibitory activity. The 40-fold loss in potency of the *N*-methyl analogue **23** relative to **22** (Table 2) can be readily explained from the crystal structure as resulting from the loss of hydrogen bonding to the enzyme. Analogue **24** was found to be equipotent to analogue **22**. The striking difference between analogues **23** and **24** was that *N*-methylpyrazole **23**, although not as potent, was found to be quite selective over all the other cathepsins B, H, L, S, and V.

Encouraged by the results of enhanced selectivity of analogue **23**, a series of N-substituted ketoamides were prepared. Increase in the steric bulk at this position gave analogues **25** to **35**. These analogues maintain relatively constant cathepsin K inhibitory activity (Table 2). All the analogues exhibited increased selectivity relative to pyrazole **22**. Constrained analogues of the isopropyl **26**, particularly cyclobutyl **30**, cyclopentyl **31**, and cyclohexyl **32** gave us highly selective inhibitors with analogues **30** and **32** being over a 100 fold selective over all the other cathepsins tested. The six-membered aryl analogues **33** to **35** are not as broadly selective as the saturated rings such as cyclohexyl analogue **32**. Since selectivity versus cathepsins S and V had proven difficult in this ketoamide series, these results were quite gratifying. The additional selectivity exhibited by these compounds is difficult to rationalize from structural data based on the similarities of the S′ subsites in these cathepsins. The enzymes would have to breathe to allow these inhibitors in a similar binding mode. Alternatively, they may bind in a different rotamer conformation. It is also possible that accommodation of these inhibitors in the S′ subsites results in shifts in binding in other subsites that are less favorable for cathepsin L, S, and V. Substitution at other positions of the pyrazole ring were also investigated. The steric probes **36** to **39** maintained similar activity to the parent pyrazole **22**, but did not offer increases in selectivity. Indazole **40**, a conformationally constrained analogue of compound **38**, did not give any significant boost in potency, indicating that favorable entropic effects of restricting internal rotors might be offset by unfavorable enthalpic effects that could not be attributed to specific ligand−protein interactions or lack thereof.[23] Although a thorough electronic effects study on analogues of pyrazole **22** was not done, several analogues (**41** to **43**) were synthesized. No dramatic improvements over pyrazole **22** were evident.

Pharmacokinetic Analysis. One of the major challenges in optimizing a peptidomimetic lead is achieving the desired physiochemical properties which will enable delivery of an orally bioavailable drug having good pharmacokinetic properties. Most of these inhibitors met Lipinski's criteria and were profiled in several in vitro pharmacokinetic predictive assays.[24] The pharmacokinetic and efflux properties of the P′ heterocyclic analogues are presented in Table 3. These compounds were characterized by excellent cell permeability in the Madin−Darby canine kidney cell monolayer transport assay. Many also had acceptable solubilities in the simulated intestinal fluid (SIF) to allow absorption. Unfortunately, analogues **19**, **20**, and **23** showed higher rates of in vitro S9 instability. Some of these analogues also exhibited plasma instability, the exception being the N-substituted pyrazoles such as **23**. Despite these limitations, pharmacokinetic properties of several analogues were evaluated in rats (Table 4). The more soluble analogues such as pyridine **14** and pyrazole **22** exhibited good oral bioavailabilities (%F = 58 and 41, respectively), while the other analogues had moderate bioavailabilities (%F = 15−28). Pyrazole **22** had a very high rate of clearance (exceeding the hepatic blood flow for rat), extremely long terminal half-life (700 min) and very high volume of distribution (V_{ss} = 15 L/kg). Introduction of an *N*-methyl group (analogue **23**) lowered the clearance rate (CL = 26 mL/min/kg) by blocking the cleavage of the amide bond next to the pyrazole and/or preventing phase II conjugation. The half-life and volume were also lower. Analogues **14**, **19**, and **20** were more moderately cleared than pyrazole **22**.

Table 2. Inhibitory Potencies (IC_{50}) vs Human Cathepsins K, L, S, V, H, B and Rat Cathepsin K

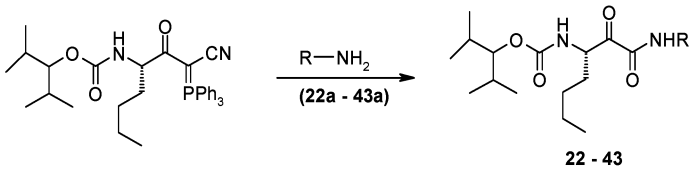

Cmpd	Structure (R)	K (IC50 nM)	L/K*	S/K*	V/K*	H/K*	B/K*	Rat Cat. K (IC50 nM)
22	 **22a**	0.77	40	3.0	21	30	670	13
23	 **23a**	32	250	91	50	>400	>400	1,700
24	 **24a**	0.41	56	7.8	29	ND	>610	11
25	 **25a**	26	220	43	4.2	>490	>490	1,500
26	 **26a**	17	260	78	66	>760	>760	1,000
27	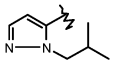 **27a**	39	260	59	120	>320	>320	2,700
28	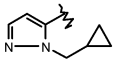 **28a**	27	220	41	63	>470	>470	1,700
29	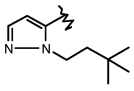 **29a**	62	68	13	46	>200	>200	1,600
30	 **30a**	15	290	130	140	>830	>830	1,100
31	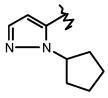 **31a**	20	190	55	71	ND	>630	1,100
32	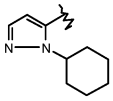 **32a**	22	190	140	130	>560	>560	1,200
33	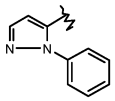 **33a**	15	250	69	65	>820	>820	790
34	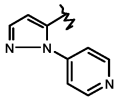 **34a**	25	44	5.4	19	>500	>500	470
35	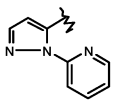 **35a**	62	40	8.3	19	ND	>200	1,200
36	 **36a**	0.47	26	1.7	14	2,100	1,100	5.5

Table 2 (Continued)

Cmpd	Structure (R)	K (IC50 nM)	L/K*	S/K*	V/K*	H/K*	B/K*	Rat Cat. K (IC50 nM)
37	 **37a**	0.71	ND	4.6	ND	ND	ND	ND
38	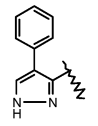 **38a**	0.21	25	4.1	9.1	1,700	1,200	1.8
39	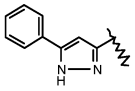 **39a**	0.65	25	7.0	20	18	520	12
40	 **40a**	0.26	ND	2.3	ND	ND	ND	ND
41	 **41a**	0.91	ND	3.6	ND	ND	ND	ND
42	 **42a**	1.7	ND	3.6	ND	ND	ND	ND
43	 **43a**	0.24	ND	4.2	ND	ND	ND	ND

* Represents selectivity ratios over the other cathepsins (e.g. L/K = IC_{50} cat L/IC_{50} cat K).

Table 3. In Vitro Data for P′ Ketoamides

Cmpd	R	Sol (SIF) (mg/mL)[a]	MDCK (nm/s) (P_{APP})[b]	Rat S9 (%)[c]	CLogP
14		1.0	210	63	5.0
22		0.27	480	77	4.6
23		0.064	490	99	4.6
19		0.074	230	98	4.8
20		0.035	N.D.	96	3.6
36		0.33	370	68	4.8

[a] Simulated intestinal fluid solubility assay, pH = 6.8 phosphate buffer with isoosmotic KCl, lethicin, and sodium taurocholate. [b] Madin−Darby canine kidney cell monolayer transport assay.[c] Rat S9 liver slice metabolism assay, % metabolized after 1 h incubation at 37 °C in duplicates.

Encouraged by the acceptable pharmacokinetic parameters for orally dosing several of these ketoamide inhibitors, it was decided to profile some in a suitable rodent pharmacodynamic model of osteoporosis. These ketoamide inhibitors were found to be less potent inhibitors of the rat cathepsin K ortholog despite high amino acid sequence identity (88%). Presumably, this difference arises from a substitution of ^{133}Ser in the rat ortholog for ^{133}Ala in the human S2 pocket.[25] Pyrazole **22**, the most potent rat cathepsin K inhibitor with good pharmacokinetic parameters, was selected for evaluation. Analogue **22** was prescreened in an ex vivo model before its evaluation in an in vivo setting. Several methods have been described in the literature to study bone resorption in an ex vivo model.[26] Since neonatal rat calvaria are an excellent source of live bone tissue and have been well documented as a bone organ culture model system, analogue **22** was evaluated in the rat calvaria assay. In Figure 2, bone resorption was stimulated with the addition of parathyroid hormone (PTH) followed by the addition of compound **22** at 1, 3, and 10 μM. A decrease in the efflux of calcium and deoxypyridinoline was obtained in a dose-dependent manner. In fact, the 10 μM dose of compound **22** completely reversed the stimulation of resorption brought about by PTH, bringing the efflux of calcium and deoxypyridinoline back to around the level of nonstimulated calvaria. Having proved the effective anti-resorptive properties of compound **22** ex vivo, it was decided to test this compound in our in vivo assay.

A PTH-stimulated hypercalcemia model, the thyroparathyroidectomized (TPTX) rat assay, was used to monitor inhibition of osteoclastic resorption. In this model, removal of the parathyroid gland results in a precipitous drop in serum calcium levels. Blood ionized

Table 4. Rat Pharmacokinetic Data for P′ Ketoamides

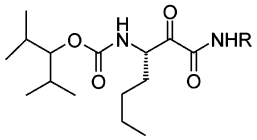

Cmpd	R	AUC_{PO} (ng·h/mL)[a]	Cl_{total} (L/min/kg)	Vss (mL/kg)	$t_{1/2}$ (min)	C_{max} (ng/mL)	t_{max} (min)	F (%)
14		2,700	36	1.2	130	1,400	15	58
22		1,100	68	15	700	370	15	41
23		1,800	26	2.0	240	970	38	28
19		750	41	3.5	130	170	10	18
20		920	28	0.65	170	690	38	15

[a] Compounds were dosed in solutol/citrate buffer, pH 3.5 (concn = 2.5 mg/mL): Plasma drug levels were determined by LC-MS/MS.

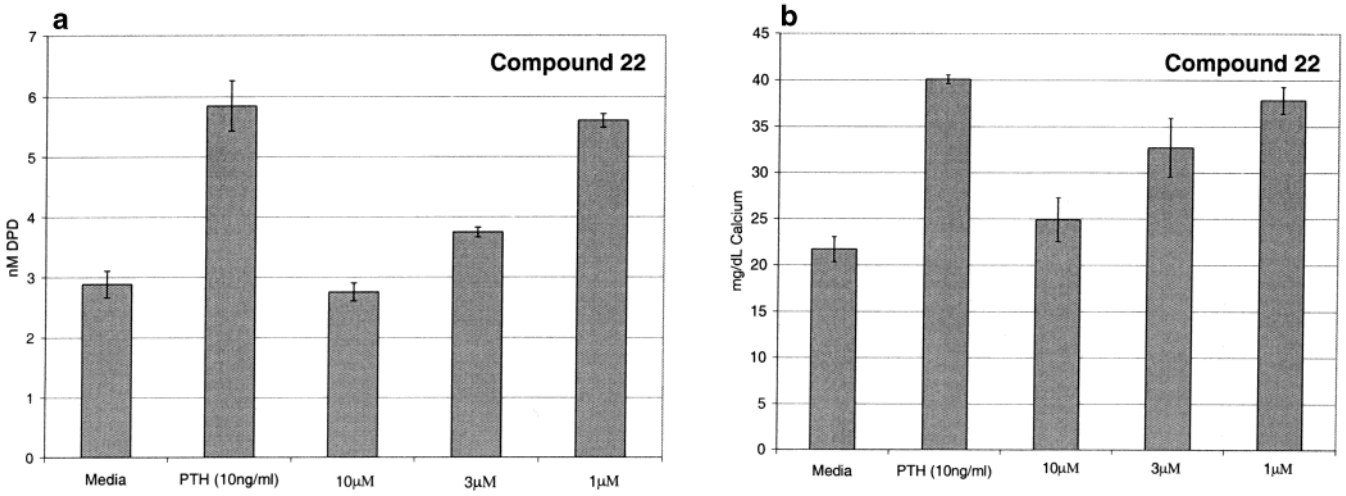

Figure 2. Deoxypyridinoline (a) and ionized calcium (b) levels from calvaria of 1−2 day old Wistar rats incubated with h-PTH (1−34), 10 ng/mL or vehicle only, and compound **22** added at 1, 3, and 10 μM concentrations. Error bars represent standard error of the mean.

calcium levels are increased significantly by infusion of 30 μg/kg/h hPTH (1−34). Codosing cathepsin K inhibitor **22** (25 mg/kg po) with PTH (30 μg/kg/h infusion) attenuates the PTH-stimulated increase in serum calcium by blocking collagen matrix degradation and subsequently inhibiting dissolution of hydroxyapatite from bone (Figure 3).

Conclusion

Modifications of the P1 and P′ regions were explored starting from a potent, ketoamide cathepsin K inhibitor. In the process of exploring these heterocyclic P′ variations, it was discovered that N-substituted pyrazoles such as analogue **23** had increased selectivity over other cathepsins tested. Exploitation of this region resulted in very selective (>100 fold) and potent cathepsin K inhibitors such as analogues **30** and **32**. A set of these ketoamides exhibited good oral bioavailabilities. Encouraged by the good oral pharmacokinetics properties of these ketoamides, a representative example, compound **22**, was used in PTH-stimulated rat calvaria bone resorption assay to monitor inhibition of osteoclastic resorption. Pyrazole **22** was also found to be efficacious in attenuating hypercalcemia in the TPTX rat model. The excellent in vitro potency and selectivity profile of several compounds described, combined with their pharmacokinetic profile, suggests that these compounds may represent a viable lead series in the discovery of new therapies for the treatment of osteoporosis.

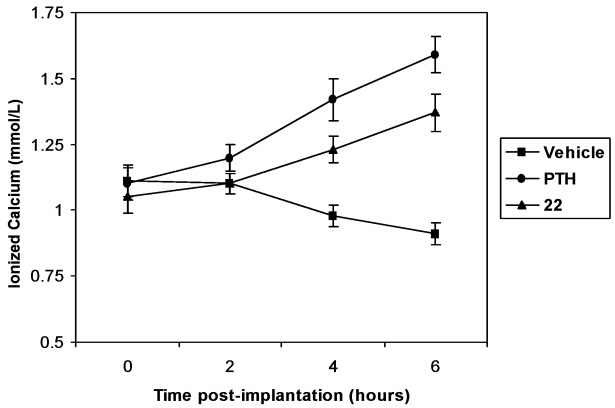

Figure 3. Ionized calcium levels of male CD TPTX rats receiving h-PTH (1−34), 30 μg/kg/h, sc via minipump or h-PTH and compound **22** administered orally 1 h prior to PTH. Compound **22** was dosed orally at 25 mg/kg in 0.5% methyl cellulose suspension at a concentration of 5 mg/mL. Error bars represent standard error of the mean.

Experimental Section

Chemistry. General Methods. Melting points were determined using a Thomas-Hoover melting point apparatus and are uncorrected. Unless stated otherwise, reagents were obtained from commercial sources and were used directly. Reactions involving air- or moisture-sensitive reagents were carried out under a nitrogen atmosphere. If not specified, reactions were carried out at ambient temperature. Silica gel (EM Science, 230−400 mesh) was used for chromatographic purification unless otherwise indicated. Anhydrous solvents were obtained from Aldrich (Sure Seal). ^{1}H NMR spectra were recorded on a Varian spectrometer; chemical shifts are reported in parts per million (ppm) relative to TMS. The following abbreviations are used to describe peak patterns when appropriate: b = broad, s = singlet, d = doublet, t = triplet, q = quartet, m = multiplet. High performance liquid chromatography (HPLC) was performed on a Beckman 126 with a Beckman 166 UV Detector (monitoring at 215 nm) with a Rainin Dynamax-60A column using a gradient consisting of 20/80 A:B to 10/90 A/B over 20 min, where A = 1% aqueous trifluoroacetic acid (TFA), B = 1% TFA in CH_3CN. Elemental analyses, performed by Atlantic Microlab, Inc. Norcross, GA, were within 0.4% of the theoretical values calculated for C, H, and N.

Methyl *N*-[(1-Isopropyl-2-methylpropoxy)carbonyl]-L-norleucinate (4). To a solution of 18 mL (129 mmol) of 2,4-dimethyl-3-pentanol **3** in 150 mL of THF was added 81.5 mL (155 mmol) of 20% phosgene in toluene at 0 °C. The reaction was stirred at rt overnight. THF was removed and the chloroformate intermediate in toluene was directly used in the next step.

To the intermediate chloroformate was added 50 mL of THF followed by 23.4 g (129 mmol) of norleucine methyl ester hydrochloride and 67.5 mL (387 mmol) of Hunig's base at 0 °C. The reaction was stirred at rt overnight. Solvent was removed and water was added. The aqueous layer was extracted with ether three times, and the combined ether layer was washed with brine and dried over magnesium sulfate. After removal of the solvent, column chromatography with hexane:ethyl acetate (10:1) as eluent provided 32 g of product **4** in 86% yield. ^{1}H NMR (300 MHz, $CDCl_3$) ppm: 5.12 (br, 1H), 4.36 (m, 2H), 3.71 (s, 3H), 1.23−1.89 (m, 8H), 0.84−0.92 (m, 15H).

1-Isopropyl-2-methylpropyl (1*S*)-1-[cyano(triphenylphosphoranylidene) acetyl]pentylcarbamate (5). To a solution of 6 g (21 mmol) of methyl *N*-[(1-isopropyl-2-methylpropoxy)carbonyl]-L-norleucinate **4** in 30 mL of THF was added 28 mL (28 mmol) of 1 M lithium hydroxide. The reaction was stirred at rt overnight. Water was added, and the solution was acidified with 1 N hydrochloric acid to around pH = 3. The mixture was extracted with ether three times, and the combined ether layer was washed with brine. After removal of the solvent, the residue was redissolved in 30 mL of dichloromethane, and 5.2 g (27 mmol) of EDC, 6.6 g (22 mmol) of (triphenylphosphoranylidene)acetonitrile, and 256 mg (2.1 mmol) of DMAP were added. The reaction was stirred at rt overnight. The reaction was diluted with 100 mL of dichloromethane, and this organic layer was washed three times with brine and dried over magnesium sulfate. After removal of solvent, column chromatography with hexane:ethyl acetate (1:1) gave 8.5 g of product **5** in 73% yield. ^{1}H NMR (300 MHz, $CDCl_3$) ppm: 7.52−7.70 (m, 15H), 5.40 (d, J = 8.0 Hz, 1H), 4.90 (m, 1H), 4.42 (t, J = 6.0 Hz, 1H), 1.20−2.08 (m, 8H), 0.86−0.95 (m, 15H).

General Procedure for the Preparation of Compounds 6−43. Ozone was bubbled through a solution of 1-isopropyl-2-methylpropyl (1*S*)-1-[cyano(triphenylphosphoranylidene)-acetyl]pentylcarbamate **5** (1 mmol) dissolved in 25 mL of dichloromethane at −78 °C for 15 min until the solution turned blue. The solution was purged with a stream of nitrogen for 5 min, and then the amine as a solution in 2 mL of dichloromethane was added. The solution was stirred at −78 °C for 15 min and then warmed to room temperature. It was concentrated, and 5 mL of a 1 M solution of silver nitrate in tetrahydrofuran:water (4:1) was added. The resulting mixture was stirred for 16 h at room temperature and then extracted with dichloromethane. The extract was washed with saturated aqueous sodium chloride. It was then dried over anhydrous magnesium sulfate, filtered, and concentrated. The residue was purified by silica gel column chromatography.

1-Isopropyl-2-methylpropyl 2,3-dioxo-3-[(thien-2-ylmethyl)-amino]propylcarbamate (6): ^{1}H NMR (300 MHz, $CDCl_3$) ppm: 7.26 (d, J = 6 Hz, 1H), 6.93−7.01 (m, 2H), 4.65 (m, 3H), 4.42 (m, 1H), 1.87 (m, 2H), 0.88(m, 12H). Anal. C, H, N.

1-Isopropyl-2-methylpropyl (1*S*)-1-methyl-2,3-dioxo-3-[(thien-2-ylmethyl)amino]propylcarbamate (7): ^{1}H NMR (300 MHz, $CDCl_3$) ppm: 7.26 (d, J = 4.1 Hz, 1H), 7.18 (br, 1H), 6.95−7.01 (m, 2H), 5.20 (br, 1H), 4.66 (br, 2H), 4.41 (m, 1H), 1.89 (m, 2H), 1.47 (d, J = 7.0 Hz, 3H), 0.88 (m, 12H). Anal. C, H, N.

1-Isopropyl-2-methylpropyl (1*S*)-1-isopropyl-2,3-dioxo-3-[(thien-2-ylmethyl)amino]propylcarbamate (8): ^{1}H NMR (400 MHz, $CDCl_3$) ppm: 7.26 (d, J = 5.9 Hz, 1H), 7.19 (br, 1H), 6.96−7.01(m, 2H), 5.27(d, J = 9.0 Hz, 1H), 5.08 (dd, J = 9.2, 4.8 Hz, 1H), 4.65 (d, J = 6.0 Hz, 2H), 4.40 (t, J = 6.0 Hz, 1H), 2.42 (m, 1H), 1.87 (m, 2H), 1.05 (d, J = 6.8 Hz, 3H), 0.87 (m, 15H). Anal. C, H, N.

1-Isopropyl-2-methylpropyl (1*S*)-3-methyl-1-{oxo[(thien-2-ylmethyl)amino]acetyl}butylcarbamate (9): ^{1}H NMR (400 MHz, $CDCl_3$) ppm: 7.25 (d, J = 6.4 Hz, 1H), 7.17 (br, 1H), 6.95−7.01 (m, 2H), 5.15 (br, 1H), 4.64 (d, J = 5.7 Hz, 2H), 4.38 (br, 1H), 1.76−1.88 (m, 4H), 1.42 (m, 1H), 1.04(d, J = 6.0 Hz, 3H), 0.96 (d,J = 6.4 Hz, 3H), 0.87 (m, 12H). Anal. C, H, N.

1-Isopropyl-2-methylpropyl (1*S*,2*S*)-2-methyl-1-{oxo-[(thien-2-ylmethyl)amino]acetyl}butylcarbamate (10): ^{1}H NMR (400 MHz, $CDCl_3$) ppm: 7.26 (d, J = 5.5 Hz, 1H), 7.19 (br, 1H), 6.95−7.00 (m, 2H), 5.28 (d, J = 8.8 Hz, 1H), 5.04 (dd, J = 9.3, 5.5 Hz, 1H), 4.66 (m, 2H), 4.39 (br, 1H), 2.17 (br, 1H), 1.87 (m, 2H), 1.33 (br, 1H), 1.13 (m, 1H), 1.00 (d, J = 6.8 Hz, 3H), 0.87 (m, 15H). Anal. C, H, N.

1-Isopropyl-2-methylpropyl (1*S*)-1-cyclohexylmethyl-2,3-dioxo-3-[(thien-2-ylmethyl)amino]propylcarbamate (11): ^{1}H NMR (300 MHz, $CDCl_3$) ppm: 7.25 (d, J = 6.0 Hz, 1H), 7.19 (br, 1H), 6.95−7.00 (m, 2H), 5.18 (m, 2H), 4.64 (d, J = 5.5 Hz, 2H), 4.39 (m, 1H), 1.03−1.98 (m, 15H), 0.88 (m, 12H). Anal. C, H, N.

1-Isopropyl-2-methylpropyl (1*S*)-2,3-dioxo-1-phenyl-3-[(thien-2-ylmethyl)amino]propylcarbamate (12): ^{1}H NMR (300 MHz, $CDCl_3$) ppm: 6.97−7.29 (m, 8H), 5.44 (m, 1H), 5.22 (br, 1H), 4.70 (m, 2H), 4.37 (t, J = 6.5 Hz, 1H), 1.84 (m, 2H), 0.85 (d, J = 7.0 Hz, 6H), 3.14−3.40 (m, 2H), 0.83(d, J = 6.9 Hz, 6H). Anal. C, H, N.

1-Isopropyl-2-methylpropyl (1*S*)-1-{oxo[(thien-2-ylmethyl)amino]acetyl}pentylcarbamate (13): ^{1}H NMR

(400 MHz, $CDCl_3$) ppm: 6.92−7.30 (m, 4H), 5.21 (br, 1H), 5.13 (br, 1H), 4.65 (s, 2H), 4.39 (br, 1H), 1.80−2.05 (m, 3H), 1.30−1.66 (m, 5H), 0.88 (m, 15H). Anal. C, H, N.

1-Isopropyl-2-methylpropyl (1*S*)-1-[oxo(pyridin-2-ylamino)acetyl]pentylcarbamate (14): ^{1}H NMR (300 MHz, $CDCl_3$) ppm: 9.30 (s, 1H), 8.39 (d, J = 4.4 Hz, 1H), 8.27 (d J = 8.2 Hz, 1H), 7.79 (m, 1H), 7.16 (m, 1H), 5.30 (br, 2H), 4.43 (t, J = 5.9 Hz, 1H), 1.38−2.08 (m, 8H), 0.91 (m, 15H). Anal. C, H, N.

1-Isopropyl-2-methylpropyl (1*S*)-1-[oxo(pyridin-3-ylamino)acetyl]pentylcarbamate (15): ^{1}H NMR (300 MHz, $CDCl_3$) ppm: 8.91 (s, 1H), 8.77 (s, 1H), 8.45 (br, 1H), 8.26 (d, J = 7.5 Hz, 1H), 7.35 (br, 1H), 5.21−5.29 (m, 2H), 4.42 (br, 1H), 1.43−2.07 (m, 8H), 0.90 (br, 15H). Anal. C, H, N.

1-Isopropyl-2-methylpropyl (1*S*)-1-[oxo(pyrazin-2-ylamino)acetyl]pentylcarbamate (16): ^{1}H NMR (400 MHz, $CDCl_3$) ppm: 9.53 (s, 1H), 9.22 (br, 1H), 8.39 (s, 1H), 8.30 (s, 1H), 5.18 (m, 2H), 4.35 (br, 1H), 1.32−2.00 (m, 8H), 0.86 (m, 15H). Anal. C, H, N.

1-Isopropyl-2-methylpropyl (1*S*)-1-[oxo(quinolin-2-ylamino)acetyl]pentylcarbamate (17): ^{1}H NMR (400 MHz, $CDCl_3$) ppm: 9.37 (s, 1H), 8.39 (d, J = 9.0 Hz, 1H), 8.19 (d,J = 9.0 Hz, 1H), 7.85 (d, J = 8.6 Hz, 1H), 7.78 (d, J = 8.2 Hz, 1H), 7.67 (m, 1H), 7.58 (m, 1H), 5.26 (m, 1H), 5.21 (br, 1H), 4.37 (t, J = 5.9 Hz, 1H), 1.20−2.10 (m, 8H), 0.86 (m, 15H). Anal. C, H, N.

1-Isopropyl-2-methylpropyl (1*S*)-1-[(isoquinolin-3-ylamino)(oxo)acetyl]pentylcarbamate (18): ^{1}H NMR(300 MHz, $CDCl_3$) ppm: 9.40 (s, 1H), 9.08 (s, 1H), 8.66 (s, 1H), 7.98 (d, J = 8.0 Hz, 1H), 7.90 (d, J = 8.1 Hz, 1H), 7.73 (br, 1H), 7.58 (br, 1H), 5.33 (br, 2H), 4.46 (br, 1H), 1.20−2.20 (m, 8H), 0.93 (m, 15H). Anal. C, H, N.

1-Isopropyl-2-methylpropyl (1*S*)-1-[oxo(1,3-thiazol-2-ylamino)acetyl]pentylcarbamate (19): ^{1}H NMR (300 MHz, $CDCl_3$) ppm: 12.48 (br, 1H), 7.80 (d, J = 2.2 Hz, 1H), 7.14(d, J = 2.2 Hz, 1H), 5.29 (m, 2H), 4.43 (m, 1H), 1.29−2.08 (m, 8H), 0.91 (m, 15H). Anal. C, H, N.

1-Isopropyl-2-methylpropyl (1*S*)-1-[oxo(1,3,4-thiadiazol-2-ylamino)acetyl]pentylcarbamate (20): ^{1}H NMR (300 MHz, $CDCl_3$) ppm: 8.99 (s, 1H), 7.30 (s, 1H), 5.23 (br, 2H), 4.41 (br, 1H), 1.40−2.05 (m, 8H), 0.90 (m, 15H). Anal. C, H, N.

1-Isopropyl-2-methylpropyl (1*S*)-1-[(isoxazol-3-ylamino)(oxo)acetyl]pentylcarbamate (21): ^{1}H NMR (300 NMR, $CDCl_3$) ppm: 9.72 (br, 1H), 8.40 (s, 1H), 7.13 (s, 1H), 5.24 (br, 2H), 4.42 (br, 1H), 1.42−2.01 (m, 8H), 0.90 (m, 15H). Anal. C, H, N.

1-Isopropyl-2-methylpropyl (1*S*)-1-[oxo(1*H*-pyrazol-5-ylamino)acetyl]pentylcarbamate (22): ^{1}H NMR (300 MHz, DMSO-d_6) ppm: 10.86 (s, 1H), 7.68 (s, 1H), 7.50 (d, J = 8.0 Hz, 1H), 6.53 (s, 1H), 4.85 (m, 1H), 4.27 (t, J = 6.1 Hz, 1H), 1.34−1.82 (m, 8H), 0.80 (m, 15H). Anal. C, H, N.

1-Isopropyl-2-methylpropyl (1*S*)-1-[[(1-methyl-1*H*-pyrazol-5-yl)amino](oxo)acetyl]pentylcarbamate (23): ^{1}H NMR (300 MHz, $CDCl_3$) ppm: 7.97 (s, 1H), 5.98 (br, 2H), 5.27 (br, 1H), 5.18 (br, 1H), 4.40 (m, 1H), 3.63 (s, 3H), 1.21−2.00 (m, 8H), 0.90 (m, 15H). Anal. C, H, N.

1-Isopropyl-2-methylpropyl (1*S*)-1-[[(1-methyl-1*H*-pyrazol-3-yl)amino](oxo)acetyl]pentylcarbamate (24): ^{1}H NMR (300 MHz, $CDCl_3$) ppm: 9.24 (s, 1H), 7.32 (d, J = 2.0 Hz, 1H), 6.75 (d, J = 2.0 Hz, 1H), 5.27 (m, 2H), 4.43 (m, 1H), 1.29−2.08 (m, 8H), 0.91 (m, 15H). Anal. C, H, N.

1-Isopropyl-2-methylpropyl (1*S*)-1-[[(1-ethyl-1*H*-pyrazol-5-yl)amino](oxo)acetyl]pentylcarbamate (25): ^{1}H NMR (400 MHz, $CDCl_3$) ppm: 7.90 (s, 1H), 5.86 (br, 2H), 5.21 (d, J = 8.1 Hz, 1H), 5.1(m, 1H), 4.33 (t, J = 6.0 Hz, 1H), 3.87 (q, J = 7.3 Hz, 2H), 1.36 (t, J = 7.3 Hz, 3H), 1.20−2.00 (m, 8H), 0.83 (m, 15H). Anal. C, H, N.

1-Isopropyl-2-methylpropyl (1*S*)-1-[[(1-Isopropyl-1*H*-pyrazol-5-yl)amino](oxo)acetyl]pentylcarbamate (26): ^{1}H NMR (300 MHz, $CDCl_3$) ppm: 8.00 (s, 1H), 5.92 (br, 2H), 5.28 (br, 1H), 5.17 (br, 1H), 4.42 (t, J = 6.0 Hz, 1H), 4.21 (m, 1H), 1.51 (d, J = 7.4 Hz, 6H), 0.90 (m, 15H). Anal. C, H, N.

1-Isopropyl-2-methylpropyl (1*S*)-1-[[(1-isobutyl-1*H*-pyrazol-5-yl)amino](oxo)acetyl]pentylcarbamate (27): ^{1}H NMR (400 MHz, $CDCl_3$) ppm: 7.92 (s, 1H), 5.82 (br, 2H), 5.21 (d, J = 8.0 Hz, 1H), 5.10 (m, 1H), 4.34 (t, J = 6.0 Hz, 1H), 3.61 (d, J = 7.3 Hz, 2H), 2.19 (m, 1H), 1.20−2.00 (m, 8H), 0.90 (m, 18H). Anal. C, H, N.

1-Isopropyl-2-methylpropyl (1*S*)-1-[{[1-(cyclopropylmethyl)-1*H*-pyrazol-5-yl]amino}(oxo)acetyl]pentylcarbamate (28): ^{1}H NMR (300 MHz, $CDCl_3$) ppm: 7.98 (s, 1H), 6.13 (s, 1H), 5.29 (m, 1H), 5.20 (m, 1H), 4.40 (t, J = 5.8 Hz, 1H), 3.82 (d, J = 6.6 Hz, 2H), 1.20−2.00 (m, 9H), 0.89 (m, 15H), 0.66 (m, 2H), 0.42 (m, 2H). Anal. C, H, N.

1-Isopropyl-2-methylpropyl (1*S*)-1-[{[1-(3,3-dimethylbutyl)-1*H*-pyrazol-5-yl]amino}(oxo)acetyl]pentylcarbamate (29): ^{1}H NMR (300 MHz, $CDCl_3$) ppm: 7.97 (s, 1H), 5.92 (br, 2H), 5.31 (d, J = 8.2 Hz, 1H), 5.17 (br, 1H), 4.41 (m, 1H), 3.90 (t, J = 8.4 Hz, 2H), 1.2−2.0 (m, 10H), 1.01 (s, 9H), 0.89 (m, 15H). Anal. C, H, N.

1-Isopropyl-2-methylpropyl (1*S*)-1-[[(1-cyclobutyl-1*H*-pyrazol-5-yl)amino](oxo)acetyl]pentylcarbamate (30): ^{1}H NMR (400 MHz, $CDCl_3$) ppm: 7.93 (s, 1H), 5.79 (br, 2H), 5.21 (d, J = 8.0 Hz, 1H), 5.09 (br, 1H), 4.37 (m, 1H), 2.64 (m, 2H), 2.37 (m, 2H), 1.2−2.0 (m, 10H), 0.83 (m, 15H). Anal. C, H, N.

1-Isopropyl-2-methylpropyl (1*S*)-1-[[(1-cyclopentyl-1*H*-pyrazol-5-yl)amino](oxo)acetyl]pentylcarbamate (31): ^{1}H NMR (300 MHz, $CDCl_3$) ppm: 7.98 (s, 1H), 5.86 (s, 2H), 5.30 (d, J = 8.4 Hz, 1H), 5.17 (m, 1H), 4.42 (t, J = 6.0 Hz, 1H), 4.32 (m, 1H), 1.23−2.20 (m, 16H), 0.90 (m, 15H). Anal. C, H, N.

1-Isopropyl-2-methylpropyl (1*S*)-1-[[(1-cyclohexyl-1*H*-pyrazol-5-yl)amino](oxo)acetyl]pentylcarbamate (32): ^{1}H NMR (400 MHz, $CDCl_3$) ppm: 7.91 (s, 1H), 5.76 (s, 2H), 5.21 (d, J = 8.2 Hz, 1H), 5.08 (m, 1H), 4.34 (t, J = 6.1 Hz, 1H), 3.66 (m, 1H), 1.20−1.99 (m, 18H), 0.82 (m, 15H). Anal. C, H, N.

1-Isopropyl-2-methylpropyl (1*S*)-1-{oxo[(1-phenyl-1*H*-pyrazol-5-yl)amino]acetyl}pentylcarbamate (33): ^{1}H NMR (300 MHz, $CDCl_3$) ppm: 8.16 (s, 1H), 7.30−7.60 (m, 5H), 6.17 (s, 2H), 5.33 (d, J = 8.0 Hz, 1H), 5.17 (m, 1H), 4.42 (m, 1H), 1.28−2.07 (m, 8H), 0.90 (m, 15H). Anal. C, H, N.

1-Isopropyl-2-methylpropyl (1*S*)-1-{oxo[(1-pyridin-4-yl-1*H*-pyrazol-5-yl)amino]acetyl}pentylcarbamate (34): ^{1}H NMR (400 MHz, $CDCl_3$) ppm: 8.73 (d, J = 5.3 Hz, 2H), 8.16 (s, 1H), 7.51 (d, J = 5.3 Hz, 2H), 6.38 (s, 2H), 5.20 (d, J = 7.7 Hz, 1H), 5.06 (br, 1H), 4.33 (br, 1H), 1.20−2.00 (m, 8H), 0.83 (m, 15H). Anal. C, H, N.

1-Isopropyl-2-methylpropyl (1*S*)-1-{oxo[(1-pyridin-2-yl-1*H*-pyrazol-5-yl)amino]acetyl}pentylcarbamate (35): ^{1}H NMR (400 MHz, $CDCl_3$) ppm: 8.33 (d, J = 4.4 Hz, 1H), 8.09 (s, 1H), 7.90 (d, J = 8.2 Hz, 1H), 7.79 (m, 1H), 7.14 (m, 1H), 5.27 (d, J = 7.9 Hz, 1H), 5.10 (m, 1H), 4.34 (t, J = 6.9 Hz, 1H), 1.20−2.00 (m, 8H), 0.83 (m, 15H). Anal. C, H, N.

1-Isopropyl-2-methylpropyl (1*S*)-1-[[(4-methyl-1*H*-pyrazol-5-yl)amino](oxo)acetyl]pentylcarbamate (36): ^{1}H NMR (400 MHz, $CDCl_3$) ppm: 9.21 (s, 1H), 7.30 (s, 1H), 5.26 (br, 1H), 5.16 (br, 1H), 4.36 (br, 1H), 2.01 (s, 3H), 1.33−1.83 (m, 8H), 0.84 (m, 15H). Anal. C, H, N.

1-Isopropyl-2-methylpropyl (1*S*)-1-[[(3-methyl-1*H*-pyrazol-5-yl)amino](oxo)acetyl]pentylcarbamate (37): ^{1}H NMR (400 MHz, $CDCl_3$) ppm: 11.51 (br, 1H), 6.61 (s, 1H), 5.23 (br, 1H), 5.14 (br, 1H), 4.36 (br, 1H), 2.32 (s, 3H), 1.34−2.01 (m, 8H), 0.85 (m, 15H). Anal. C, H, N.

1-Isopropyl-2-methylpropyl (1*S*)-1-{oxo[(4-phenyl-1*H*-pyrazol-5-yl)amino]acetyl}pentylcarbamate (38): ^{1}H NMR (400 MHz, $CDCl_3$) ppm: 9.14 (s, 1H), 7.66 (s, 1H), 7.28−7.43 (m, 5H), 5.31 (s, 1H), 5.13 (br, 1H), 4.34 (br, 1H), 1.20−2.02 (m, 8H), 0.82 (m, 15H). Anal. C, H, N.

1-Isopropyl-2-methylpropyl (1*S*)-1-{oxo[(3-phenyl-1*H*-pyrazol-5-yl)amino]acetyl}pentylcarbamate (39): ^{1}H NMR (300 MHz, $CDCl_3$) ppm: 7.70 (d, J = 7.4 Hz, 2H), 7.46 (m, 3H), 7.19 (s, 1H), 5.33 (d, J = 7.5 Hz, 1H), 5.19 (br, 1H), 4.41 (m, 1H), 1.38−2.15 (m, 8H), 0.87 (m, 15H). Anal. C, H, N.

1-Isopropyl-2-methylpropyl (1*S*)-1-[[(4-fluoro-1*H*-indazol-3-yl)amino](oxo)acetyl]pentylcarbamate (40): ^{1}H

NMR (300 MHz, $CDCl_3$) ppm: 9.43 (s, 1H), 7.36 (br, 2H), 6.81 (m, 1H), 5.36 (br, 2H), 4.47 (br, 1H), 1.20−2.20 (m, 8H), 0.94 (m, 15H). Anal. C, H, N.

1-Isopropyl-2-methylpropyl (1*S*)-1-[[(4-cyano-1*H*-pyrazol-5-yl)amino](oxo)acetyl]pentylcarbamate (41): ^{1}H NMR (300 MHz, $CDCl_3$) ppm: 9.80 (s, 1H), 7.92 (s, 1H), 5.31 (d, J = 7.7 Hz, 1H), 5.12 (m, 1H), 4.40 (br, 1H), 1.30−2.10 (m, 8H), 0.93 (m, 15H). Anal. C, H, N.

Ethyl 5-[((3S)-3-{[(1-Isopropyl-2-methylpropoxy)carbonyl]amino}-2-oxoheptanoyl)amino]-1*H*-pyrazole-4-carboxylate (42): ^{1}H NMR (400 MHz, $CDCl_3$) ppm: 10.65 (s, 1H), 7.85 (s, 1H), 5.26 (br, 1H), 5.14 (m, 1H), 4.32 (m, 3H), 1.36 (t, J = 7.0 Hz, 3H), 1.20−2.00 (m, 8H), 0.83 (m, 15H). Anal. C, H, N.

1-Isopropyl-2-methylpropyl (1*S*)-1-[[(4-bromo-1*H*-pyrazol-5-yl)amino](oxo)acetyl]pentylcarbamate (43): ^{1}H NMR (400 MHz, $CDCl_3$) ppm: 8.93 (s, 1H), 7.5 (s, 1H), 5.15 (m, 2H), 4.35 (br, 1H), 1.23−2.05 (m, 8H), 0.84 (m, 15H). Anal. C, H, N.

Rat Calvaria Assay. Calvaria was surgically removed from 1 to 2 day old Wistar rats and placed in a sterile centrifuge tube containing BGJb media (Fitton-Jackson Modification), GIBCO BRL with penicillin (10 U/mL)/streptomycin (10 μg/mL). In a tissue culture hood, calvaria were washed 2× with fresh media, trimmed of any excess tissue attached to the calvaria, and placed in fresh media. The calvaria were cut using a 8 mm keyhole punch to give circular calvaria pieces of uniform size and were then placed into wells of a 48-well tissue culture plate containing 0.4 mL of BGJb media containing 1 mg/mL BSA and penicillin (10 U/mL)/streptomycin (10 μg/mL). Calvaria were then incubated for 24 h at 37 °C, 5% CO_2 on a Nutator rotator prior to treatment. Media was aspirated and replaced with 0.4 mL of fresh media containing designated concentration of PTH (10 ng/mL media) or vehicle only. Vehicle is 4mM acetic acid/1 mg/mL BSA. Cultures were incubated for 24 h, retreated daily as described, for a total treatment time of 48 h. Upon completion of the assay, the 24−48 h media is collected in tubes and stored at −20 °C until analysis is performed. Calvaria were air-dried for several days, and dry weight was quantitated on a Mettler balance if needed. PTH, IL1, and PGE2 have been shown to stimulate bone resorption in in vitro rat neonatal calvaria assays and are utilized as controls in this assay. Resorption is measured in three ways: (1) quantitation of calcium in the supernatant by atomic emission spectroscopy (ICPE); (2) quantitation of calcium in the supernatant by a colorimetric assay; (3) quantitation of deoxypyridinoline in the supernatant by ELISA (Metra DPD EIA Kit, Catalog #8007, Quidel Corp.). Deoxypyridinoline is released as a byproduct of collagen degradation by the osteoclast.

TPTX Protocol. Male CD rats weighing 275−300 g, Charles River Research Laboratory (Raleigh, NC), were received and allowed one week to acclimate to the facility. Animals had free access to water and were maintained on a normal diet and light cycle. Following the acclimation period, animals were anesthetized and a thyroparathyroidectomy performed. Forty-eight hours post TPTX, animals were anesthetized and a blood sample collected via the tail vein to measure serum calcium concentration to verify successful TPTX and randomize the animals into treatment groups. For administration of PTH, 30 μg/kg/h, animals were anesthetized and an osmotic pump implanted sc to initiated PTH infusion. To evaluate the anti-resorptive effect of test compounds, the compounds were given at different times depending upon route of administration. Compounds administered orally were given an hour prior to implantation. Compounds administered sc, iv, or ip were either coadministered or administered 2 h postimplant. To measure the compound's ability to block the increase in serum calcium, rats were anesthetized 2, 4, and 6 h postinfusion and a blood sample collected via tail vein. After the 6 h bleed, animals were euthanized.

Crystallization. Activated cathepsin K was complexed with a 10-fold molar excess of inhibitor and concentrated to ∼2 mg/mL. Crystals were grown by the hanging drop vapor diffusion method at room temperature. Protein was mixed with an equal volume of reservoir buffer containing 0.2 M $(NH_4)_2SO_4$ and 30% PEG8000. Prior to data collection, glycerol was added to 25%, and the crystals were flash frozen in a stream of liquid nitrogen.

Diffraction data was collected on an RAXIS4 area detector operating on a Rigaku rotating anode generator. The crystals diffracted to 2.2 Å resolution and belonged to the space group P1 with cell dimensions a = 31.63 Å, b = 72.86 Å, c = 78.47 Å, α = 90.42°, β = 90.28°, γ = 90.16°. The data were processed with DENZO and SCALEPACK. The data were 83% complete with a R_{merge} of 6.5%. The structure was solved by molecular replacement using coordinates 1EF7 from the PDB databank and CNX. The structure was refined to a R_{factor} of 20.9%. In the final model, all residues lie within the allowed regions of the Ramachandran plot with rms deviations in the bonds and angle of 0.008 Å and 1.6°, respectively.

Biological Data. All assays for cathepsin K were carried out with human and rat recombinant enzyme. Assays for cathepsins S and V were also carried out with human recombinant enzyme. Assays for human cathepsins B, H, and L were carried out with enzyme, purchased from Athens Research and Technology, Inc., prepared from human liver tissue. Standard assay conditions for the determination of kinetic constants used a fluorogenic peptide substrate, typically (5*S*,8*S*)-13-amino-5-benzyl-13-imino-3-methylene-*N*-(4-methyl-2-oxo-2*H*-chromen-7-yl)-6-oxo-1-phenyl-2-oxa-4,7,12-triazatridecane-8-carboxamide (Cbz-Phe-Arg-AMC) and were determined in 100 mM sodium acetate at pH 5.5 containing 10 mM dithiothreitol and 120 mM sodium chloride. A stock substrate solution of Cbz-Phe-Arg-AMC was prepared at a concentration of 50 mM in dimethyl sulfoxide. This substrate was diluted into the assay for a final substrate concentration of 10 μM in the rat cathepsin K, human cathepsin K, and human cathepsin B assays; a final substrate concentration of 5 μM in the human cathepsin L assay; and a final substrate concentration of 2 μM in the human cathepsin V assay. The K_m value for Cbz-Phe-Arg-AMC on rat cathepsin K is 27 μM, on human cathepsin K is 70 μM, on human cathepsin B is 400 μM, on human cathepsin L is 2.7 μM and on human cathepsin V is 32 μM.

A stock substrate solution of benzyl (1*S*)-1-{[((1*S*)-1-{[((1*S*)-4-{[amino(imino)methyl]amino}-1-{[(4-methyl-2-oxo-2*H*-chromen-7-yl)amino]carbonyl}butyl)amino]carbonyl}-2-methylpropyl)amino]carbonyl}-2-methylpropylcarbamate (Cbz-Val-Val-Arg-AMC) was prepared at a concentration of 10 mM in dimethyl sulfoxide. This substrate was diluted into the assay for a final substrate concentration of 10 μM in the human cathepsin S assay. The K_m value for Cbz-Val-Val-Arg-AMC on human cathepsin S is >100 μM.

A stock substrate solution of (2*S*)-2-amino-5-{[amino(imino)-methyl]amino}-*N*-(2-naphthyl)pentanamide hydrochloride (L-Arg-β-naphthalamide·HCl) was prepared at a concentration of 10 mM in dimethyl sulfoxide. This substrate was diluted into the assay for a final substrate concentration of 50 μM in the cathepsin H assay. The K_m value for L-Arg-*b*-naphthalamide·HCl on cathepsin H is 195 μM.

All assays contained 10% dimethyl sulfoxide. Independent experiments found that this level of dimethyl sulfoxide had no effect on kinetic enzymatic constants. All assays were conducted at 30 °C. Product fluorescence (excitation at 360 nm; emission at 440 nm (except cathepsin H which used excitation at 340 nm; emission at 420 nm)) was monitored with a PerSeptive Biosystems Cytofluor II fluorescence plate reader. Product progress curves were generated over 2.3 h monitoring the formation of 7-amino-4-methylcoumarin product (or β-naphthalamide for cathepsin H).

Cathepsin K Activation. The proform of cathepsin K was converted to mature cathepsin K by brief exposure to pH 4 in the presence of 5 mM L-cysteine. Typically, 5 mM L-cysteine was added to 10 mL of approximately 1 mg/mL procathepsin K. One milliliter of this solution was diluted 10-fold into 450 mM sodium acetate at pH 4.0 containing 5 mM L-cysteine. This solution was reacted at 23°C for 2 min before neutralization

with 2 mL of 1.8 M sodium acetate at pH 6.0. The neutralized sample was added to the remaining 9 mL of procathepsin K. The mixture was incubated at 4 °C for 2−3 days. The activated cathepsin K was chromatographed on a Poros HS II column as described above.

Inhibition Studies. Potential inhibitors were evaluated using the progress curve method. Assays were carried out in the presence of variable concentrations of test compound. Reactions were initiated by addition of buffered solutions of inhibitor and substrate to enzyme. Data analysis was conducted according to one of two procedures depending on the appearance of the progress curves in the presence of inhibitors. For those compounds whose progress curves were linear, the enzymatic activity (RATE) was plotted against the concentration of test compound, including inhibitor concentration of zero ([I] = 0), and the IC_{50} determined from a fit of eq 1 to the data,

$$\text{rate } V_{max}/(1 + ([I]/\ IC_{50})) \quad (1)$$

where V_{max} is the best fit estimate of the maximal enzymatic activity. K_i values were calculated from IC_{50} values using eq 2 assuming a competitive model.

$$K_i = IC_{50} \times \left[1 - \frac{S}{(S + K_m)}\right] \quad (2)$$

For those compounds whose progress curves showed downward curvature characteristic of time-dependent inhibition, the data from individual sets was analyzed using the computer program DynaFit (Kuzmic, P. *Anal. Biochem*. **1996**, *237*, 260−273) to give K_i values according to the following kinetic mechanism:

$$E + S \leftrightarrows ES$$

$$ES \rightarrow E + P$$

$$E \rightarrow EX$$

$$E + I \leftrightarrows EI$$

Pharmacokinetic Studies in Rats. Male Han Wistar rats (weight range: 225−300 g) were anesthetized with isofluorane and surgically prepared with jugular vein and femoral vein cannulas (oral rats had only jugular cannulas) 2 days before dosing. On the prior day of dosing, each compound was dissolved in 15% solutol/citrate buffer/0.1% ascorbic acid, pH 3.5. Rats were dosed intravenously into the femoral vein at a level of 5 mg/kg or orally at 10 mg/kg. Blood samples were collected prior to dosing and at 0.03, 0.25, 0.5, 0.75, 1, 1.5, 2.5, 4, 6, 8, and 24 h postdosing from the jugular vein cannula into unheparinized syringes. The blood was clotted on ice and centrifuged to obtain serum and frozen until analysis. Serum samples were prepared by protein precipitation with acetonitrile containing an internal standard. Compound analysis was by turboionspray on a Sciex API III+ using multiple reaction monitoring. Samples were chromatographed using a Phenomenex Luna C18 column (30 × 2 mm, 3m) at ambient temperature using a gradient (20−95%) with 10 mM ammonium acetate (pH 4.0) and methanol mobile phases at a flow rate of 0.20 mL/min. Data reduction was performed using Sciex MacQuan software. Noncompartmental methods were used to calculate pharmacokinetic parameters from the resulting serum concentration vs time profiles using WinNonLin.

Acknowledgment. The authors wish to thank Randy Rutkowski, Robert Johnson, and Peter Kitrinos for analytical support.

References

(1) (a) Marcus, R.; Feldman, D.; Kelsey, J. In *Osteoporosis*, 1st ed.; Academic Press: New York, 1996. (b) Baron, R. Anatomy and Ultrastructure of Bone. In *Primer on the Metabolic Bone Diseases and Disorders of Mineral Metabolism*, 1st ed.; Favus, M. J., Ed.; American Society for Bone and Mineral Research: Kelseyville, CA, 1990; pp 3−9.

(2) (a) Broemme, D.; Okamoto, K. Human cathepsin O2, a novel cysteine protease highly expressed in osteoclastomas and ovary. Molecular cloning, sequencing and tissue distribution. *Biol. Chem. Hoppe-Seyler* **1995**, *376*, 379−384. (b) Drake, F. H.; Dodds, R. A.; James, I. A.; Connor, J. R.; Debouck, C.; Richardson, S.; Lee-Rykaczewski, L.; Coleman, L.; Riemann, D.; Barthlow, R.; Hastings, G.; Gowen, M. Cathepsin K, but not cathepsins B, L or S is abundantly expressed in human osteoclasts. *J. Biol. Chem*. **1996**, *271*, 12511−12516. (c) Littlewood-Evans, A.; Kokubo, T.; Ishibashi, O.; Inaoka, T.; Wlodarski, B.; Gallagher, J. A.; Bilbe, G. Localization of cathepsin K in human osteoclasts by in situ hybridization and immunohistochemistry. *Bone* **1997**, *20*, 81−86. (d) Shi, G.-P.; Chapman, H. A.; Bhairi, S. M.; DeLeeuw, C.; Reddy, V. Y.; Weiss, S. J. Molecular cloning of human cathepsin O, a novel endoproteinase and homologue of rabbit OC2. *FEBS Lett*. **1995**, *357*, 129−134.

(3) Inui, T.; Ishibashi, O.; Inaoka, T.; Origane, Y.; Kumegawa, M.; Kokubo, T.; Yamaura, T. Cathepsin K antisense oligodeoxynucleotide inhibits osteoclastic bone resorption. *J. Biol. Chem*. **1997**, *272*, 8109−8112.

(4) (a) Gelb, B. D.; Moissoglu, K.; Zhang, J.; Martignetti, J. A.; Broemme, D.; Desnick, R. J. Cathepsin K: isolation and characterization of the murine cDNA and genomic sequence, the homologue of the human pycnodysostosis gene. *Biochem Mol. Med*. **1996**, *59*, 200−206. (b) Johnson, M. R.; Polymeropoulos, M. H.; Vos, H. L.; Oritz de Luna, R. I.; Francomano, C. A. A nonsense mutation in the cathepsin K gene observed in a family with pycnodysostosis. *Genome Res*. **1996**, *6*, 1050−1055. (c) Gelb, B. D.; Shi, G.-P.; Chapman, H. A.; Desnick, R. J. Pycnodysostosis, a lysosomal disease caused by cathepsin K deficiency. *Science* **1996**, *273*, 1236−1238. (d) Motyckova, G.; Fisher, D. Pycnodysostosis: role and regulation of cathepsin K in osteoclast function and human disease. *Curr. Mol. Med*. **2002**, *2* (5), 407−421.

(5) (a) Saftig, P.; Hunziker, E.; Wehmeyer, O.; Jones, S.; Boyde, A.; Rommerskirch, W.; Detlev, J. D.; Schu, P.; von Figura, K. Impaired osteoclastic bone resorption leads to osteopetrosis in cathepsin K deficient mice. *Proc. Natl. Acad. Sci. U.S.A*. **1998**, *95*, 13453−13458. (b) Gowen, M.; Lazner, F.; Dodds, R.; Kapadia, R.; Field, J.; Tavaria, M.; Bertoncello, I.; Drake, F.; Zavarselk, S.; Tellis, I.; Hertzog, P.; Debouck, C.; Kola, I. Cathepsin K knockout mice develop osteopetrosis due to a deficit in matrix degradation but not demineralization. *J. Bone Miner. Res*. **1999**, *14*, 1654−1663.

(6) (a) James, I. E.; Marquis, R. W.; Blake, S. M.; Hwang, S. M.; Gress, C. J.; Ru, Y.; Zembryki, D.; Yamashita, D. S.; McQueney, M. S.; Tomaszek, T. A.; Oh, H. J.; Gowen, M.; Veber, D. F.; Lark, M. W. Potent and Selective Cathepsin L Inhibitors Do Not Inhibit Osteoclast Resorption in vitro. *J. Biol. Chem*. **2001**, *276* (15), 11507−11511. (b) Stroup, G. B.; Lark, M. V.; Veber, D. F.; Bhattacharya, A.; Blake, S.; Dare, L. C.; Erhard, K. F.; Hoffman, S. J.; James, I. E.; Marquis, R. W.; Ru, Y.; Vasko-Moser, J. A.; Smith, B. R.; Tomaszek, T.; Gowen, M. Potent and selective inhibition of human cathepsin K leads to inhibition of bone resorption in vivo in a nonhuman primate. *J. Bone Miner. Res*. **2001**, *16* (10), 1739−1746.

(7) Hashimoto, Y.; Kakegawa, H.; Narita, Y.; Hachiya, Y.; Hayakawa, T.; Kos, J.; Turk, V.; Katunuma, N. Significance of cathepsin B accumulation in synovial fluid of rheumatoid arthritis. *Biochem. Biophys. Res. Commun*. **2001**, *283* (2), 334−339. (b) Szpaderska, A. M.; Frankfater, A. An intracellular form of Cathepsin B contributes to invasiveness in cancer. *Cancer Res*. **2001**, *61* (8), 3493−3500. (c) Greenspan, P. D.; Clark, K. L.; Tommasi, R. A.; Cowen, S. D.; McQuire, L. W.; Farley, D. L.; Van Duzer, J. H.; Goldberg, R. L.; Zhou, H.; Du, Z.; Fitt, J. J.; Coppa, D. E.; Fang, Z.; Macchia, W.; Zhu, L.; Michael, P. Identification of dipeptidyl nitriles as potent and selective inhibitors of cathepsin B through structure-based drug design. *J. Med. Chem*. **2001**, *44*, 4524−4534.

(8) (a) Turk, B.; Turk, D.; Turk, V. Review: Lysosomal cysteine proteases: more than scavengers. *Biochim. Biophys. Acta* **2000**, 1477 (1−2), 98−111. (b) Buhling, F.; Fengler, A.; Brandt, W.; Welte, T.; Ansorge, S.; Nagler, D. K. Review: Novel cysteine proteases of the papain family. *Adv. Exp. Med. Biol*. **2000**, *477*, 241−254.

(9) Turk, V.; Turk, B.; Turk, D. Review: Lysosomal cysteine proteases: facts and opportunities. *EMBO J*. **2001**, *20* (17), 4629−4633.

(10) (a) Yamashita, Dennis S.; Dodds, Robert A. Cathepsin K and the design of inhibitors of cathepsin K. *Current Pharmaceutical Design* **2000**, *6* (1), 1−24. (b) Leung, D.; Abbenante, G.; Fairlie, D. Protease inhibitors: current status and future prospects. *J. Med. Chem*. 2000, *43*, 305−341. (b) Schirmeister, T.; Otto, H. Cysteine proteases and their inhibitors. *Chem Rev*. **1997**, *97*, 133−171.

(11) Votta, B. J.; Levy, M. A.; Badger, A.; Bradbeer, J.; Dodds, R. A.; James, I. E.; Thompson, S.; Bossard, M. J.; Carr, T.; Conner, J. R.; Tomaszek, T. A.; Szewczuk, L.; Drake, F. H.; Veber, D. F.;

Gowen, M. Peptide aldehyde inhibitors of cathepsin K inhibit bone resorption both in vitro and in vivo. *J. Bone Miner. Res.* **1997**, *12*, 1396−1406. (b) Yasuma, T.; Oi, S.; Choh, N.; Nomura, T.; Furuyama, N.; Nishimura, A.; Fujisawa, Y.; Sohda, T. Synthesis of peptide aldehyde derivatives as selective inhibitors of human cathepsin L and their inhibitory effect on bone resorption. *J. Med. Chem.* **1998**, *41*, 4301−4308. (c) Karanewsky, D. S.; Bai, X.; Linton, S. D.; Krebs, J. F.; Wu, J.; Pham, B.; Tomaselli, K. J. Conformationally constrained inhibitors of caspase-1 (interleukin-1â converting enzyme) and of the human CED-3 homologue caspase-3 (CPP32, apopain). *Bioorg. Med. Chem. Lett.* **1998**, *8*, 2757−2762.

(12) (a) Moon, J. B.; Coleman, R. S.; Hanzlik, R. P. Reversible covalent inhibition of papain by a peptide nitrile. ^{13}C NMR evidence for a thioimidate ester adduct. *J. Am. Chem. Soc.* **1986**, *108*, 1350−1351. (b) Brisson, J.-R.; Carey, P. R.; Storer, A. C. Benzoylamidoacetonitrile is bound as a thioimidate in the active site of papain. *J. Biol. Chem.* **1986**, *261*, 9087−9089. (c) Liang, T.-C.; Abeles, R. H. Inhibition of papain by nitriles: mechanistic studies using NMR and kinetic measurements. *Arch. Biochem. Biophys.* **1987**, *252*, 626−634.

(13) (a) Ando, R.; Morinaka, Y. A new class of proteinase inhibitor. Cyclopropenone-containing inhibitor of papain. *J. Am. Chem. Soc.* **1993**, *115*, 1174−1175. (b) Ando, R.; Sakaki, T.; Morinaka, Y.; Takahashi, C.; Tamao, Y.; Yoshii, N.; Katayama, S.; Saito, K.; Tokuyama, H.; Isaka, M.; Nakamura, E. Cyclopropenone-containing cysteine proteinase inhibitors. Synthesis and enzyme inhibitory activities. *Bioorg. Med. Chem.* **1999**, *7*, 571−579.

(14) (a) Majalli, A. M. M.; Chapman, K. T.; MacCoss, M.; Thornberry, N. A.; Peterson, E. P. Activated ketones as potent reversible inhibitors of interleukin-1α converting enzyme. *Bioorg. Med. Chem. Lett.* **1994**, *4*, 1965−1968. (b) Yamashita, D. S.; Smith, W. W.; Zhao, B.; Janson, C. A.; Tomaszek, T. A.; Bossard, M. A.; Levy, M. A.; Oh, H.-J.; Carr, T. J.; Thompson, S. T.; Ijames, C. F.; Carr, S. A.; McQueney, M.; D'Alessio, K. J.; Amegadzie, B. Y.; Hanning, C. R.; Abdel-Meguid, S.; DesJarlais, R. L.; Gleason, J. G.; Veber, D. F. Structure and design of potent and selective cathepsin K inhibitors. *J. Am. Chem. Soc.* **1997**, *119*, 11351−11352. (c) DesJarlais, R. L.; Yamashita, D. S.; Oh, H.-J.; Uzinskas, I. N.; Erhard, K. F.; Allen, A. C.; Haltwanger, R. C.; Zhao, B.; Smith, W. W.; Abdel-Meguid, S. S.; D'Allesio, K.; Janson, C. A.; McQueney, M. S.; Tomaszek, T. A.; Levy, M. A.; Veber, D. F. Use of X-ray cocrystal structures and molecular modeling to design potent and selective non-peptide inhibitors of cathepsin K. *J. Am. Chem. Soc.* **1913**, *35*, 9114−9115. (d) Marquis, R. W.; Ru, Y.; LoCastro, S. M.; Zeng, J.; Yamashita, D. S.; Oh, H.-J.; Erhard, K. F.; Davis, L. D.; Tomaszek, T. A.; Tew, D.; Salyers, K.; Proksch, J.; Ward, K.; Smith, B.; Levy, M.; Cummings, M. D.; Haltiwanger, R. C.; Trescher, G.; Wang, B.; Hemling, M. E.; Quinn, C. J.; Cheng, H.-Y.; Lin, F.; Smith, W. W.; Janson, C. A.; Zhao, B.; McQueney, M. S.; D'Alessio, K.; Lee, C.-P.; Marzulli, A.; Dodds, R. A.; Blake, S.; Hwang, S.-M.; James, I. E.; Gress, C. J.; Bradley, B. R.; Lark, M. W.; Gowen, M.; Veber, D. F. Azepanone-Based Inhibitors of Human and Rat Cathepsin K. *J. Med. Chem.* **2001**, *44*, 1380−1395.

(15) (a) Hu, L.-Y.; Abeles, R. H. Inhibition of cathepsin B and papain by peptidyl α-keto esters, α-keto amides α-diketones and α-keto acids. *Arch. Biochem. Biophys.* **1990**, *281*, 271−274. (b) Li, Z.; Patil, G. S.; Golubski, Z. E.; Hori, H.; Tehrani, K.; Foreman, J. E.; Eveleth, D. D.; Bartus, R. T.; Powers, J. C. Peptide R-keto ester, R-keto amide, and R-keto acid inhibitors of calpains and other cysteine proteases. *J. Med. Chem.* **1993**, *36*, 3472−3480. (c) Harbeson, S. L.; Abelleira, S. M.; Akiyama, A.; Barrett III, R.; Carroll, R. M.; Straub, J. A.; Tkacz, J. N.; Wu, C.; Musso, G. F. Stereospecific synthesis of peptidyl α-keto amides as inhibitors of calpain. *J. Med. Chem.* **1994**, *37*, 2918−2929.

(16) Altmann E.; Renaud, J.; Green, J.; Farley, D.; Cutting, B.; Jahnke, W. Arylaminoethyl amides as novel noncovalent cathepsin K inhibitors. *J. Med. Chem.* **2002**, *45* (12) 2352−2354.

(17) Cacciola, Joseph; Fevig, John M.; Stouten, Pieter F. W.; Alexander, Richard S.; Knabb, Robert M.; Wexler, Ruth R. Synthesis and activity studies of conformationally restricted α-ketoamide factor Xa inhibitors. *Bioorg. Med. Chem. Lett.* **2000**, *10* (11), 1253−1256.

(18) Rosenthal, K.; Karlström, A.; Undén, A. The 2,4-Dimethylpent-3-yloxycarbonyl (Doc) group as a new, nucleophile-resistant protecting group for tyrosine in solid-phase peptide synthesis. *Tetrahedron Lett.*, **1997**, *38* (6), 1075−1078

(19) Wasserman, Harry H.; Ho, Wen-Bin. (Cyanomethylene)phosphoranes as novel carbonyl 1,1-dipole synthons: An efficient synthesis of α-keto acids, esters, and amides. *J. Org. Chem.* **1994**, *59* (16), 4364−6.

(20) Dorgan, Roderick J.; Parrick, J.; Hardy, Christopher, R. The Preparation of 1-protected-1H-pyrazolo[3,4-b]pyridines and attempts to move the 1-substituent. *J. Chem. Soc., Perkin Trans.1* **1980**, 938−942.

(21) Frigola, J.; Colombo, A.; Pares, J.; Martinez, L.; Sagarra, R.; Roser, R. Synthesis, structure and inhibitory effects on cyclooxygenase, lipoxygenase, thromboxane synthetase and platelet aggregation of 3-amino-4,5-dihydro-1H-pyrazole derivatives. *Eur. J. Med. Chem. Chim. Ther.* **1989**, *24*, 435−446.

(22) Ege, G.; Franz, H. Reactions with diazoazoles Part VI. Unequivocal synthesis of 3-methyl-3H-azolotetrazoles. *J. Heterocycl. Chem.* **1982**, *18*, 1267−1273.

(23) (a) Sharp, K. Entropy-enthalpy compensation: Fact or artifact? *Protein Sci.* **2001**, *10*, 661−667. (b) Liu, L.; Guo, Q.-X. Isokinetic relationship, isoequilibrium relationship and enthalpy−entropy compensation. *Chem. Rev.* **2001**, *101*, 673−696. (c) Plake, H. R.; Sundberg T. B.; Woodward, A. R.; Martin, S. F. Design and synthesis of conformationally constrained, extended and reverse turn pseudopeptides as Grb2-SH2 domain antagonist. *Tetrahedron Lett.* **2003**, *44*, 1571−1574.

(24) Lipinski, C. A.; Lombardo, F.; Dominy, B. W.; Feeney, P. J. Experimental and computational approaches to estimate solubility and permeability in drug discovery and development settings. *Adv. Drug Delivery Rev.* **1997**, *23*, 3−25

(25) (a) Veber, D. F.; Yamashita, D. S.; Oh, H.-J.; Smith, B. R.; Salyers, K.; Levy, M.; Lee, C.-P.; Marzulli, A.; Smith, P.; Tomaszek, T.; Tew, D.; McQueney, M.; Stroup, G. B.; Lark, M. W.; James, I. E.; Gowen, M. Novel inhibitors of the osteoclast specific cysteine protease, cathepsin K. *Peptides for the New Millennium, Proceedings of the American Peptide Symposium, 16th*; June 26−July 1, 1999, Minneapolis, MN; Fields, G. B., Tam, J. P., Barany, G., Eds.; Kluwer Academic Publishers: Dordrecht, Netherlands, 2000; CODEN: 69ATHX Conference, pp 453−455. (b) McQueney, M. S.; Feild, J.; Hanning, C. R.; Brun, K.; Ramachandran, K.; Connor, J.; Drake, F.; Jones, C. S.; Amegadzie, B. Y. *Protein Expression Purif.* **1998**, *14* (3), 387−394.

(26) (a) Mundy, G. R.; Roodman, G. D.; Bonewald, L. F.; Oreffo, R. O. C.; Boyce, B. F. Assays for bone resorption and bone formation. *Methods Enzymol.* **1991**, *198* (Pept. Growth Factors, Pt. C), 502−510. (b) Hahn, T. J.; Westbrook, S. L.; Halstead, L. R. Cortisol modulation of osteoblast metabolic activity in cultured neonatal rat bone. *Endocrinology* **1984**, *114* (5), 1864−1870. (c) Conaway, H. H.; Grigorie, D.; Lerner, U. H. Differential effects of glucocorticoid on bone resorption in neonatal mouse calvariae stimulated by peptide and steroid-like hormones. *J. Endocrinol.* **1997**, *155*, 513−521.

JM030373L